The Journal of Immunology

RESEARCH ARTICLE | MARCH 15 2012

Targeting TNF-α to Neoangiogenic Vessels Enhances Lymphocyte Infiltration in Tumors and Increases the Therapeutic Potential of Immunotherapy FREE

Arianna Calcinotto; ... et. al

J Immunol (2012) 188 (6): 2687–2694.
https://doi.org/10.4049/jimmunol.1101877

Targeting TNF-α to Neoangiogenic Vessels Enhances Lymphocyte Infiltration in Tumors and Increases the Therapeutic Potential of Immunotherapy

Arianna Calcinotto,*,†,‡ Matteo Grioni,*,† Elena Jachetti,*,†,‡ Flavio Curnis,†,§ Anna Mondino,†,¶ Giorgio Parmiani,†,‖ Angelo Corti,†,§ and Matteo Bellone*,†

Abnormal tumor vasculature impairs T lymphocyte adhesion to endothelial cells and lymphocyte extravasation into neoplastic tissues, limiting the therapeutic potential of both active and adoptive immunotherapies. We have found that treatment of tumor-bearing mice with NGR-TNF, a Cys-Asn-Gly-Arg-Cys peptide-TNF fusion product capable of altering the endothelial barrier function and improving drug penetration in tumors, associated with the intratumor upregulation of leukocyte-endothelial cell adhesion molecules, the release of proinflammatory cytokines and chemokines, and the infiltration of tumor-specific effector $CD8^+$ T cells. As a result, NGR-TNF enhanced the therapeutic activity of adoptive and active immunotherapy, delaying tumor growth and prolonging survival. Furthermore, we have found that therapeutic effects of these combinations can be further increased by the addition of chemotherapy. Thus, these findings might be relevant for the design of novel immunotherapeutic approaches for cancer patients. ***The Journal of Immunology*****, 2012, 188: 2687–2694.**

Growing tumors develop strategies that directly or indirectly impair effector T lymphocyte functions (1). In addition, the hypoxic tumor microenvironment favors the formation of new vessels (i.e., neoangiogenesis) that are disorganized, tortuous, and more leaky then the normal ones. These vascular abnormalities can increase the interstitial pressure, cause heterogeneous permeability, and promote irregular blood flow (2). Furthermore, angiogenic factors such as vascular endothelial cell (EC) growth factors (VEGF) and fibroblast growth factors can cause downregulation of intracellular adhesion molecule-1/2 (ICAM-1/2), VCAM-1, and CD34 on EC, a phenomenon defined as *EC anergy* (3). Hence, the interaction of leukocytes with the endothelial lining of vessels is reduced, and effector T cells, regardless of being induced in vivo by vaccination or adoptively transferred (4, 5), may be impaired in their migration into tumor sites and cannot exert the antitumor effects necessary to eradicate the tumor (6, 7).

TNF-α is a cytokine produced in the tumor microenvironment mainly by macrophages, but also by endothelial cells and tumor cells (8). This cytokine can exert potent antitumor effects both in animal models and in patients treated by isolated limb perfusion, a regional cancer therapy used to deliver high doses of TNF into the bloodstream of a limb and to avoid severe systemic side effects (9). In this setting and depending on its dose, TNF can cause endothelial cell activation, increased vessel permeability, endothelial cell damage, and massive hemorrhagic necrosis (9). Although the administration of TNF at therapeutic doses is precluded by its severe systemic toxicity, safe and therapeutic systemic administration can be obtained by targeting TNF to angiogenic tumor vessels. For example, TNF has been fused to Cys-Asn-Gly-Arg-Cys (NGR) (10), a tumor-homing peptide that recognizes an aminopeptidase N (CD13) isoform selectively expressed by endothelial cells in tumor vessels (11, 12). The selective recognition of the endothelial lining of angiogenic tumor vessels by this peptide has also been confirmed with peptide-labeled paramagnetic quantum dots and quantitative molecular magnetic resonance imaging in tumor mouse models (13). Systemic administration of low doses of the NGR-TNF fusion protein can induce antitumor effects stronger than those elicited by similar doses of TNF (14). In addition, the delivery of ultra-low doses (e.g., picograms) of NGR-TNF to the tumor vasculature overcomes major counterregulatory mechanisms and increases the penetration of doxorubicin (DOXO) and other chemotherapy agents in murine models of lymphoma, melanoma, and spontaneous prostate cancer (15, 16). While a primary mechanism of NGR-TNF–induced drug penetration is related to disassembly of endothelial VE-cadherin dependent adherence junctions and alteration of endothelial barrier function in tumors (17), other mechanisms might also be brought into play, such as increased tumor perfusion and reduction of interstitial pressure.

NGR-TNF, either alone or in combination with chemotherapy, is currently being tested in various clinical studies in cancer patients (18, 19).

In this study, we investigated whether selective targeted delivery of NGR-TNF to tumor vessels might promote the activation of

*Cellular Immunology Unit, San Raffaele Scientific Institute, 20132 Milan, Italy; †Program of Immunology, Gene Therapy and Bio-Immunotherapy of Cancer, San Raffaele Scientific Institute, 20132 Milan, Italy; ‡Università Vita-Salute San Raffaele, 20132 Milan, Italy; §Tumor Biology and Vascular Targeting Unit, San Raffaele Scientific Institute, 20132 Milan, Italy; ¶Lymphocyte Activation Unit, San Raffaele Scientific Institute, 20132 Milan, Italy; and ‖Immuno-Biotherapy of Melanoma and Solid Tumors Unit, San Raffaele Scientific Institute, 20132 Milan, Italy

Received for publication June 24, 2011. Accepted for publication January 13, 2012.

This work was supported by grants from the Italian Association for Cancer Research (to M.B., A. Corti., A.M., and G.P.), the Ministry of Health (Rome, to M.B.), the Ministry of University and Research (Rome, to M.B. and A. Corti), and Alleanza Contro il Cancro, Programma Straordinario di Ricerca Oncologica 2006, Programma 3 (to M.B., G.P., and A. Corti). A. Calcinotto conducted this study in partial fulfillment of her Ph.D. at San Raffaele University.

Address correspondence and reprint requests to Dr. Matteo Bellone and Dr. Angelo Corti, San Raffaele Scientific Institute, via Olgettina 58, 20132 Milan, Italy. E-mail addresses: bellone.matteo@hsr.it (M.B.) and corti.angelo@hsr.it (A.C.)

The online version of this article contains supplemental material.

Abbreviations used in this article: DC, dendritic cell; DLI, donor lymphocyte infusion; DOXO, doxorubicin; EC, endothelial cell; HSCT, hematopoietic stem cell transplantation; i.d., intradermal; NGR, Cys-Asn-Gly-Arg-Cys; NGR-TNF, a CNGRCG peptide-TNF fusion product; pDLI, presensitized DLI; TBI, total body irradiation; TIL, tumor-infiltrated lymphocyte; TRAMP, transgenic adenocarcinoma of the mouse prostate; UGA, urogenital apparata; VEGF, vascular endothelial cell growth factor.

tumor-associated EC and the recruitment of effector T cells, and whether NGR-TNF could be used to ameliorate the efficacy of active or adoptive immunotherapy, alone and in combination with chemotherapy. Our results indicate that treatment of tumor-bearing mice with low doses of NGR-TNF is associated with the upregulation of endothelial cell adhesion molecules in tumor vessels and enhances the local production of immunomodulating cytokines, thereby favoring the extravasation of immune cells and improving therapeutic activity of immunotherapy.

Materials and Methods

Animals, cell lines, and reagents

Wild type C57BL/6J (Charles River Breeding Laboratories; Calco, Italy), heterozygous C57BL/6 transgenic adenocarcinoma of the mouse prostate (TRAMP) (20), C57BL/6-Tg(TcraTcrb) 1100Mjb/J (21) and B6.129S7-Rag1tm1Mom/J mice (22) were housed in a pathogen-free animal facility and treated in accordance with the European Community guidelines. The latter two lines were crossed to obtain RAG-$1^{-/-}$ OTI mice. The in vivo experiments were approved by the Ethical Committee of the Istituto Scientifico San Raffaele. B16-OVA are B16F1 melanoma cells (American Type Culture Collection) expressing the truncated form of OVA lacking the leader sequence (23). RMA is an H-2^b Rauscher virus-induced thymoma (24). Cells were maintained in RPMI 1640 with penicillin-streptomycin and 10% heat-inactivated FCS and the medium of B16-OVA cells was supplemented with hygromycin (100 μg/ml). B16F1 melanoma cells were maintained in IMDM with penicillin-streptomycin and 10% heat-inactivated FCS (Euroclone, Pero, Italy). HUVECs (Clonetics, Lonza, Switzerland) were cultured according to the recommended protocols. All experiments were performed with HUVECs at passages 1 to 4. NGR-TNF and TNF were produced and characterized as described in (14), and they were administered i.p. (5 ng/kg). DOXO was purchased from Pharmacia-Upjohn (Milan, Italy) and was administered i.p. (4 mg/kg). All drugs were diluted with 0.9% sodium chloride, containing 100 μg/ml endotoxin-free HSA (Farma-Biagini, Lucca, Italy), except for DOXO, which was diluted with 0.9% sodium chloride alone.

OTI cells

OVA-specific and in vitro-activated $CD8^+$ T (OTI) cells from RAG-$1^{-/-}$ OTI mice were obtained as previously described (25). Single-cell suspensions (1×10^6 cells/ml) of spleen and lymph nodes cells from RAG-$1^{-/-}$ OTI mice were seeded into six-well plates together with bone marrow-derived dendritic cells (DCs; ratio, 20:1) (26) loaded with 100 nM $OVA_{257–264}$ (SIINFEKL; Proimmune, Bradenton, FL) in RPMI 1640 supplemented with penicillin/streptomycin, 10 mM HEPES, 10 mM sodium-pyruvate, 50 μM 2-ME, 10% heat-inactivated FCS, and IL-12 (3.5 ng/ml; R&D Systems, Minneapolis, MN). On day 3 of culture, cells were harvested and seeded into new six-well plates together with culture medium and 50 U/ml of IL-2 (R&D Systems). At day 5, cells were labeled with CFSE as described (26), suspended in PBS, and injected into the tail vein of mice.

Immunization procedures

Tag-$IV_{404–411}$ (VVYDFLKC), $OVA_{257–264}$ (SIINFEKL), and TRP-$2_{180–188}$ (VYDFFVWLH) peptides were purchased from Research Genetics (Huntsville, AL). DCs were prepared from bone marrow as described elsewhere (26). On day 7 of culture, DCs were resuspended in PBS at 2×10^6 cells/ml and incubated for 60 min at 37°C with 2 μg/ml of the synthetic peptide. DCs were injected intradermally (i.d.) (5×10^5 cells/mouse) in the right flank.

Tumor implantation, processing, and flow cytometry analyses

Mice were challenged s.c. in the left flank with 2×10^5 B16-OVA or 5×10^4 B16F1 cells. Tumor size was evaluated by measuring two perpendicular diameters with a caliper. In survival experiments, animals were killed when the tumor became ulcerated or as indicated in the figure legends. For tumor EC analysis, 19-d-old melanomas were processed to single-cell suspension and stained with primary anti–VCAM-1, anti–ICAM-2 mAb, and secondary PE-conjugated anti-rat IgG and APC-conjugated anti-CD31 mAb (BD Biosciences). Dead cells were excluded by physical parameters or by the addition of 7-aminoactinomycin D (BD Biosciences) immediately before flow cytometric analysis.

For tumor-infiltrated lymphocytes (TIL) analysis, tumors were collected at day 14; they were disaggregated and digested in collagenase D for 1 h at 37°C to obtain single-cell suspensions. After neutralization of unspecific binding with FcR blocker (BD Pharmingen, Buccinasco, Italy), cells were stained with specific mAb and assessed for phenotype by flow cytometry. Cells were also assessed for intracellular cytokine production after stimulation with PMA/ionomycin or RMA cells pulsed with the relevant peptide as previously described (27). Samples were acquired with a FACSCanto system. Analyses were conducted with FlowJo software gating on low physical parameters that select for lymphocytes.

Combined treatments in TRAMP mice and mice bearing B16F1 melanomas

TRAMP mice were sublethally irradiated (600 rad), and the next day they were transplanted i.v. with 1×10^7 viable bone marrow cells via hematopoietic stem cell transplantation (HSCT). A donor lymphocyte infusion (DLI) consisting of 6×10^7 splenocytes was provided 2 wk later; these splenocytes were presensitized (pDLI) against the HY Ag by injection of 5×10^6 syngenic male bone marrow cells (28). The day after, mice were immunized with DCs pulsed with the immunodominant Tag epitope IV (DC-Tag-IV) as described above. Six days after the vaccination, mice were treated i.p. with NGR-TNF or TNF (5 ng/kg) and 2 h later animals were sacrificed. Their urogenital apparata (UGA) were processed for immunohistochemistry and scored on blind-coded samples by an expert pathologist as described by Hess Michelini et al. (28). Anti-CD3 (Serotec) immunodetection was performed according to the manufacturer's instructions. CD3 sections were digitally scanned (ScanScope, Aperio) and then analyzed with the Spectrum Plus software (Aperio).

Mice bearing a 6-d-old B16F1 melanoma were sublethally irradiated, and the next day they were transplanted i.v. with 6×10^7 splenocytes derived from syngenic donors presensitized 1 wk before by i.d. injection of 5×10^5 TRP-$2_{180–188}$-pulsed DCs. One week after the AT, mice were randomly assigned to either one of the following treatments (five per group): weekly i.p. injection of PBS; biweekly i.d. injection of DC-TRP-2 (5×10^5 cells/mouse) either alone or alternated by biweekly i.p. injection of TNF (5 ng/kg) followed 2 h later by DOXO (4 mg/kg); or biweekly DC-OVA injections alternated by biweekly NGR-TNF (5 ng/kg) and DOXO treatments. In addition, one group of mice received only total body irradiation (TBI) and AT, and other mice were treated with TBI followed by DC-TRP2 and the combination of NGR-TNF and DOXO.

Quantification of cytokines and chemokines into the tumor mass

One gram of tumor tissue was treated with 9 ml Lysis Buffer constituted by 50mM Tris HCl pH 7.3, 2 mM EDTA, 1:500 Protease Inhibitor Cocktail Set III (Calbiochem; Gibbstown, NJ). The tumor tissue was homogenized with a mixer and centrifuged at 13,000 × *g* for 10 min at 4°C. The supernatant was recovered and stored at −80°C. Analysis of soluble molecules was conducted with Mouse CytokineMAP B version 1.0 by Rules Based Medicine (Austin, TX).

Immunofluorescence

Tumors were embedded in Killik frozen section medium (Bio-Optica, Milan, Italy) for quick freezing. Cryostatic sections (6 μm thick) were prepared, adsorbed on polylysine-coated slides, fixed for 30 min with PBS containing 4% paraformaldehyde. Detection of endothelial cells was done as follows: tissue sections were incubated with 150 μl PBS containing 1% BSA, 0.1% Triton X-100 (PBS-BT), and 5% normal goat serum for 1 h at room temperature. The solution was then removed and replaced with PBS-BT containing APC-conjugated anti-CD31 mAb MEC-13.3 (1:100) and FITC-conjugated anti-CD8 (1:100) and then incubated for 1 h at room temperature. The slides were rinsed again and incubated for 5 min with PBS containing 0.1 μg/ml DAPI (Sigma) to stain cell nuclei. Sections were examined under a microscope (Carl Zeiss, Axioscop 40FL; original magnification ×630).

Analysis of ICAM-1 expression on HUVEC

Five × 10^5 HUVEC were detached with trypsin-EDTA, washed, and immediately incubated with TNF or NGR-TNF at various concentrations for 1.5 h on ice. After washing, cells were resuspended in culture medium, incubated for 16 h at 37°C, 5% CO_2, and stained with primary mouse anti-human ICAM-1 and secondary goat anti-mouse (BD Biosciences). Samples were acquired with a FACSCanto system and DEVA sotware, and data were analyzed using FlowJo software.

In vitro cytolytic assay

B16F1 cells were cultured in 96-well flat-bottom plates with TNF or NGR-TNF (100 ng/ml, 6×10^4 cells per 100 μl) in DMEM complete medium containing 2 μg/ml actinomycin D (200 μl/well, 9 × 6-well plate). After

20 h at 37°C, 5% CO_2, the cytotoxic activity was quantified by standard MTT assay (29).

Statistics

Statistical analyses were performed with unpaired Student *t* test or Student *t* test followed by Wilcoxon posttest. Survival curves were compared using the log rank test; p values < 0.05 were considered statistically significant.

Results

NGR-TNF transiently modifies the tumor microenvironment by inducing upregulation of leukocyte-adhesion molecules on endothelial cells, release of cytokines or chemokines, and infiltration by functional CD8$^+$ T cells

TNF activates ECs and increases vessel permeability (9). To investigate the effect of NGR-TNF on ECs, we designed an in vitro assay in which the binding phase is limited to 1.5 h on ice. Then the unbound reagent is washed away and cells are incubated overnight to quantify the effects of bound TNF on cells. Therefore, we incubated CD13$^+$ HUVECs (30) with NGR-TNF or TNF and measured the cell surface expression of ICAM-1, a molecule involved in leukocyte adhesion and transmigration (31). Both TNF and NGR-TNF induced dose-dependent expression of ICAM-1 on HUVECs (Fig. 1A); however, NGR-TNF was more effective at each dose tested (Fig. 1B).

Tumor cells may express CD13, but they should not express the isoform recognized by NGR-TNF (12). Therefore, we investigated whether B16 melanoma cells expressed CD13 and, more importantly, were targeted by NGR-TNF. As shown in Fig. 1C, B16 melanoma cells expressed CD13, although the commercially available mAb did not allow to identify the specific isoform. When added to the culture medium, both NGR-TNF and TNF did not kill melanoma cells, even at 10 ng/ml, and when combined with DOXO they did not increase the DOXO-mediated cytotoxicity (Fig. 1D). Thus, NGR-TNF does not appear to have a direct effect on tumor cells.

To verify whether NGR-TNF administration can induce the upregulation of adhesion molecules also on ECs of tumor vessels, we exploited the well-characterized (23) and well-vascularized (32) B16-OVA model. Therefore, mice bearing well-established s.c. B16-OVA melanoma (i.e., 126.3 $\pm$ 8.6 mm^2 $\pm$ SEM; $n = 17$) were infused i.v. with in vitro-activated OVA-specific OTI cells to follow a sizeable population of tumor-reactive T cells. Two days later NGR-TNF, TNF, or PBS was injected i.p. Based on previous reports of the most effective combination between NGR-TNF and chemotherapy (15, 16), tumors were excised after an additional 2 h and processed to study VCAM-1 and ICAM-2 expression on CD31$^+$ endothelial cells, or they were homogenized and analyzed for the presence of soluble cytokines. NGR-TNF administration induced the upregulation of both VCAM-1 and ICAM-2 on CD31$^+$ cells (Fig. 1E, 1F, respectively) and local release of several cytokines and chemokines (Fig. 1G). In particular MIP-2, MCP-1/CCL-2, MCP-3/CCL-7, oncostatin-M, and stem cell factor were significantly increased following NGR-TNF administration (Fig. 1G).

Having found that within 2 h NGR-TNF causes EC activation and local release of proinflammatory cytokines and chemokines, we investigated whether this might favor T cells infiltration into the tumor. Therefore, activated CFSE-labeled OTI cells were adoptively transferred into mice bearing a 12-d-old melanoma, and 2 d later mice (mean diameter 53.7 $\pm$ 7.3 mm^2 $\pm$ SEM, $n = 15$) were treated with NGR-TNF, TNF, or PBS. After an additional 2 h, mice were sacrificed and the tumors were collected and analyzed by flow cytometry. At that time, the tumor mass of NGR-TNF–treated mice was characterized by a consistent infiltrate of CD8$^+$ cells localized in close proximity to the vessels or dispersed among tumor cells (Supplemental Fig. 1). CD8$^+$ cells were less abundant in melanoma from PBS and TNF-treated mice (Supplemental Fig. 1). Quantification of TIL by flow cytometry confirmed that CFSE$^+$ cells were much more abundant in NGR-TNF–treated mice than in PBS- or TNF-treated mice (Fig. 2A). Consistent with the notion that NGR-TNF specifically targets CD13$^+$ neoangiogenic vessels (11, 12), CFSE$^+$ cells were equally represented in the spleen, blood, and kidney of mice treated with PBS, NGR-TNF, or TNF (Fig. 2B–D).

TIL were also assessed for phenotype and effector functions. As expected for a population of activated TCR transgenic T cells, all OTI cells were CD8$^+$CD44$^+$ (data not shown). Of note, most CFSE-labeled OTI T cells in the tumor of mice treated with NGR-TNF also produced IFN-γ (Fig. 2E, 2F).

To investigate the persistence and effector function of migrating OTI cells in NGR-TNF treated mice, some mice were sacrificed 24 h after treatment. As reported in Supplemental Fig. 2, the absolute numbers of tumor infiltrating CFSE$^+$ (Supplemental Fig. 2A) and IFN-γ$^+$ (Supplemental Fig. 2B) cells quantified at 2 and 24 h were similar, suggesting that tumor infiltration was a rather precocious and rapid event.

We also evaluated whether the phenomenon we observed in vivo with OTI cells occurred as well for nontransgenic T cells within a spontaneous cancer. We have recently reported that the infusion of alloreactive T cells overcomes tumor-specific T cell tolerance usually found in TRAMP mice (33) with autochthonous prostate cancer (20), allowing tumor debulking and increased overall survival (28). Therefore, 16-wk-old TRAMP mice were subjected to nonmyeloablative total body irradiation (600 rad) and 1 d later transplanted with 1×10^7 bone marrow cells (HSCT) derived from congenic female donors. Two weeks after the HSCT, mice received a DLI of 6×10^7 splenocytes derived from congenic females previously sensitized against male Ag (pDLI) (28). One day after the pDLI, mice were vaccinated with DC–Tag-IV, and 6 d later treated with either NGR-TNF or TNF (Fig. 3A). Immunohistochemical analyses conducted 2 h after the last treatment showed that the infusion of NGR-TNF favored infiltration of donor-derived CD3$^+$ cells within the prostate tumors (Fig. 3B). Quantification of prostate tumor sections indicated that the number of CD3$^+$ cells in prostate tumors was significantly higher in NGR-TNF-treated mice when compared with TNF-treated ones (Fig. 3C). Thus, targeting TNF to tumor vessel increases T cell infiltration of both transplantable and autochthonous tumors.

The combination of NGR-TNF and adoptive immunotherapy increases the survival of melanoma-bearing mice

Having found that activated OTI cells performed better when combined with NGR-TNF (Fig. 2), we wished to investigate whether adoptive immunotherapy and NGR-TNF act in synergy against a growing melanoma. Preliminary experiments were conducted to identify the number of OTI cells that as a single therapeutic agent exerted a measurable effect. Activated OTI cells were tested in mice bearing an 8-d-old melanoma (Fig. 4A). In a range between 1 and 6×10^6 cells, the highest dose gave the best antitumor effect (Fig. 4B and data not shown).

Next, we tested the association between NGR-TNF treatment and adoptive transfer (Fig. 4A). Whereas TNF combined with 6×10^6 OTI cells failed to significantly delay tumor growth and to prolong mouse survival (Fig. 4B, 4C), the administration of NGR-TNF prior to T cell infusion delayed tumor development and provided a survival advantage to tumor-bearing mice (Fig. 4B, 4C). These data indicate that NGR-TNF enhances tumor infiltration by CD8 T cells and the therapeutic potential of adoptive immunotherapy.

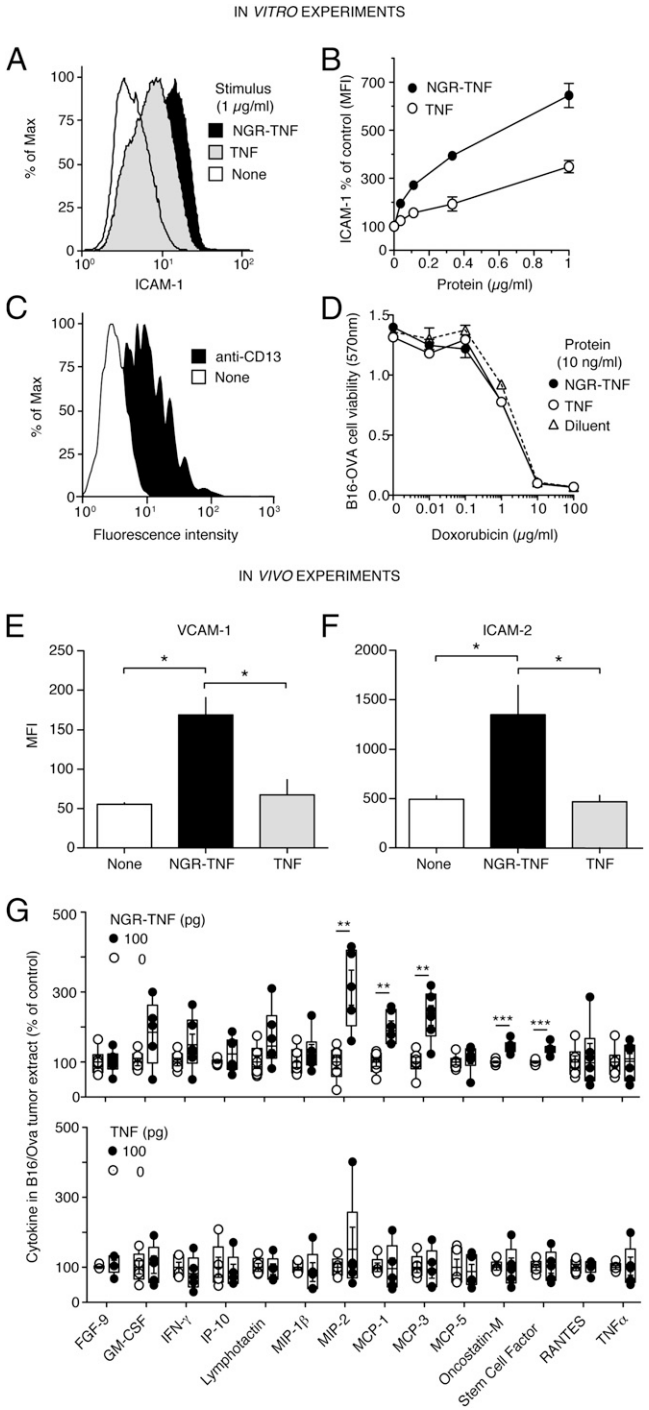

FIGURE 1. NGR-TNF treatment induces the upregulation of adhesion molecules on CD31$^+$ cells and cytokine and chemokine release in the tumor microenvironment. HUVECs were detached with trypsin-EDTA, washed, and immediately incubated with TNF or NGR-TNF solutions at various concentrations for 1.5 h on ice. After washing, the cells were resuspended in culture medium, incubated for 16 h at 37˚C, 5% CO_2, and analyzed by flow cytometry. (**A**) Fluorescence curves obtained with NGR-TNF, TNF, or no treatments. (**B**) Quantification of mean fluorescence intensity is reported. Data are representative of at least two independent experiments. (**C**) B16-OVA cells were stained with primary anti-mouse CD13 and secondary PE-conjugated anti-rat IgG2a (black histogram) or only with secondary PE-conjugated anti-rat IgG2a Ab (white histogram). (**D**) B16-OVA cells were incubated with TNF or NGR-TNF solutions at 10 ng/ml in DMEM complete medium containing 2 μg/ml actinomycin D (200 μl/well, 96-well plate). After 20 h at 37˚C, 5% CO_2, cell viability was quantified by standard MTT assay. (**E–G**) Mice were challenged s.c. with B16-OVA cells, and 19 d later they were infused i.v. with activated OTI cells (6×10^6). Two days later, NGR-TNF (5 ng/kg; $n = 3$), TNF (5 ng/kg; $n = 3$) or PBS (None; 100 μl; $n = 3$) was injected i.p. After an additional 2 h, tumors were excised and processed to single-cell suspension for flow cytometric analysis after staining with anti-CD31, anti-VCAM-1, and anti-ICAM-2 mAb. Expression of VCAM-1 (E) and ICAM-2 (F) on live CD31$^+$ cells are reported as mean (± SD) fluorescence intensity (MFI). Data are representative of three independent experiments. (G) Alternatively, the tumor tissue was homogenized and analyzed for the indicated soluble molecules by Mouse CytokineMAP B version 1.0. The graphs report the concentration of the indicated soluble molecules as a percentage of the concentration found in PBS-treated mice. Data from two independent experiments involving five to six animals per group were aggregated. Statistical analysis was performed using the Student t test: *$0.01 < p < 0.05$, **$0.001 < p < 0.01$, ***$p < 0.001$.

NGR-TNF promotes the efficacy and therapeutic activity of immunotherapy and chemoimmunotherapy

We next investigated whether NGR-TNF could also increase efficacy of active immunotherapy (vaccination) either alone or in combination with chemotherapy. To minimize the therapeutic efficacy of chemotherapy or NGR-TNF as single agents, treatment was started at day 14, when tumors had an average size of ~47 mm^2. Vaccination of mice bearing a B16-OVA melanoma was delivered by i.d. injection of DCs (26) pulsed with $OVA_{257–264}$ and biweekly boosting. NGR-TNF was administered 1 wk after DC-OVA, based on the hypothesis that NGR-TNF favors tumor infiltration by activated CTL at the peak of the vaccine-induced immune response. As expected (23), DC-OVA only modestly prolonged survival of melanoma-bearing mice (Fig. 5A), but its combination with NGR-TNF significantly prolonged overall animal survival (Fig. 5A). Of note, ~50% of NGR-TNF treated mice in combination with DC-OVA were still alive when control mice treated with DC-OVA alone or NGR-TNF alone had to be sacrificed because of tumor overgrowth (Fig. 5A).

Because immunotherapy in several instances could be combined with chemotherapy (34) and NGR-TNF has been shown to enhance tumor permeability to chemotherapeutic agents (15, 16), we next investigated the possibility that NGR-TNF administration might increase the therapeutic efficacy of chemoimmunotherapy. As a result, the DC-OVA vaccine was combined with DOXO given biweekly 2 h after NGR-TNF. The rationale was to boost the vaccine-induced immune response by causing chemotherapy-mediated tumor cell death and release of tumor-associated Ags. To establish the triple combined treatment, we started by associating NGR-TNF with DOXO. NGR-TNF, given alone (Fig. 5B) or provided 2 h before DOXO (Fig. 5B), was largely ineffective in this experimental setting, possibly because of the overt tumor growth. Likewise, the association of DC-OVA with DOXO increased mice survival (Fig. 5C), but to lower extents than those observed in mice receiving the combination of DC-OVA, NGR-TNF, and DOXO (Fig. 5D). Indeed, the triple combination further increased the overall survival of the mice (DC-OVA plus DOXO versus DC-OVA plus NGR-TNF plus DOXO; $p < 0.0001$). Delayed tumor growth in NGR-TNF–treated mice (Fig. 5D) correlated with a higher frequency of CD8$^+$ TIL (Supplemental Fig. 3) that was still evident 4 d after NGR-TNF treatment, suggesting that the effects of NGR-TNF on TIL, either direct or indirect, lasted for several days. Overall survival and tumor infiltration were lower in mice treated with DC-OVA, TNF, and DOXO (Fig. 5D, Supplemental Fig. 3), and the former was comparable to that of mice receiving DC-OVA and DOXO (Fig. 5B), thus highlighting the importance of the NGR-vascular targeting moiety.

Finally, the combined therapeutic approach was investigated in the context of an immune response specific for TRP-2, a natural tumor-

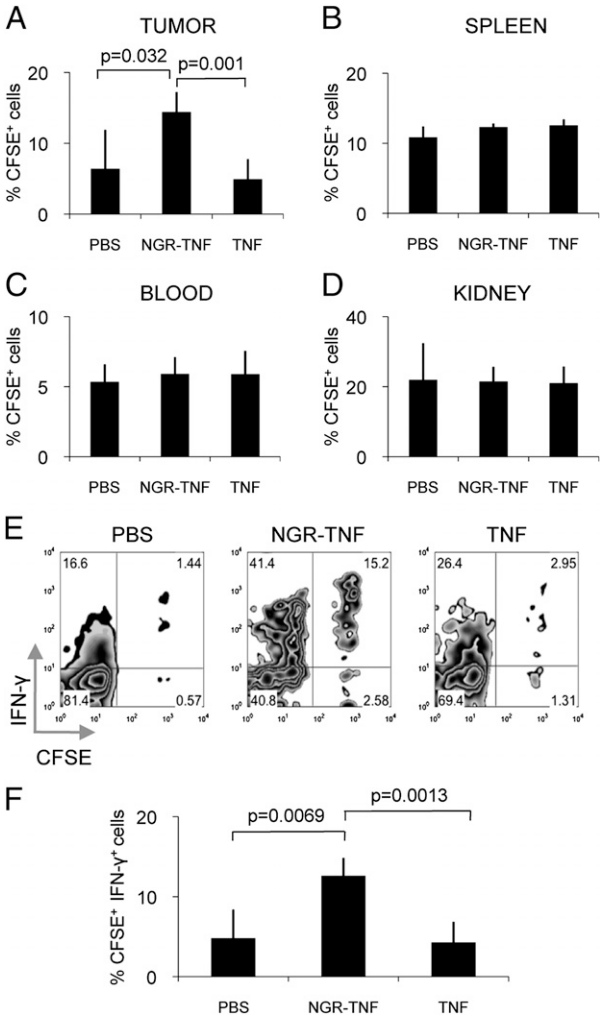

FIGURE 2. NGR-TNF treatment is associated with increased melanoma infiltration by fully functional CD8$^+$ T cells. Mice were challenged s.c. with B16-OVA cells, and 12 d later they were infused i.v. with activated and CFSE$^+$-labeled OTI cells (3×10^7). After an additional 2 d, animals were treated with PBS ($n = 5$); NGR-TNF ($n = 5$), or TNF ($n = 5$) as described in Fig. 1, and 2 h later single-cell suspensions of (**A**) tumor, (**B**) spleen, (**C**) blood, and (**D**) kidney were analyzed by flow cytometry after staining with CD8 mAb. Dead cells were excluded by physical parameters. Data are reported as a percentage ± SD of CFSE$^+$ cells within the CD8$^+$ cells. (**E**) Representative plots of TIL (gated on CD8$^+$ cells) for each experimental condition. Numbers refer to the percentage of cells in each quadrant. (**F**) Quantification of CFSE$^+$IFN-γ$^+$ TIL (gated on CD8$^+$ cells). Statistical analysis was performed using the Student *t* test. Data are representative of at least three independent experiments.

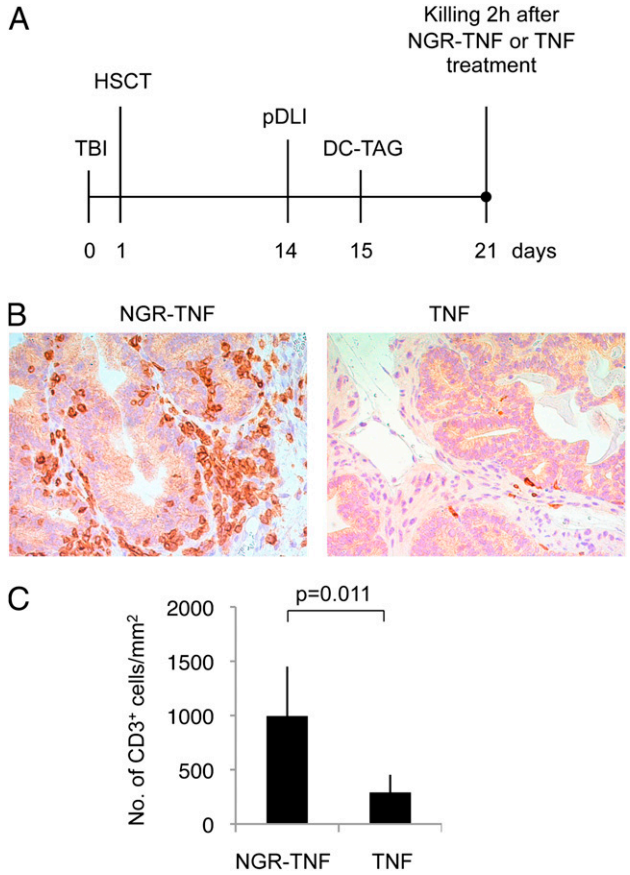

FIGURE 3. NGR-TNF treatment increases the infiltration of TIL into the prostate of TRAMP mice. Sixteen-week-old TRAMP mice were subjected to nonmyeloablative total body irradiation (600 rad) and 1 d later were transplanted with 1×10^7 bone marrow cells derived from congenic female donors. Two weeks after the transplant, mice received a DLI of 6×10^7 splenocytes derived from congenic females previously sensitized against male Ag. One day after the pDLI, mice were vaccinated with DC-Tag-IV. After 6 d, mice were treated with either NGR-TNF ($n = 6$) or TNF ($n = 6$) and killed 2 h later. See *Materials and Methods* for further experimental details. (**A**) A schematic representation of the treatment schedule. (**B**) Paraffin-embedded sections of UGA were analyzed by immunohistochemistry with anti-CD3 (Novared chromogen; original magnification ×40). (**C**) The number of CD3$^+$ cells/mm^2 obtained by the blind analysis of the entire prostate of several individual mice is shown. Data were aggregated from two independent experiments involving three animals per group.

associated Ag (23). B16 melanoma-bearing mice were sublethally irradiated and infused with splenocytes from TRP-2–sensitized C57BL/6 mice. Seven days later, the mice were vaccinated with TRP-$2_{180–188}$–pulsed DC and boosted biweekly. NGR-TNF or TNF along with DOXO were provided 1 wk after each immunization. As shown in Supplemental Fig. 4, the survival of NGR-TNF–treated mice was significantly prolonged compared with that of TNF-treated mice.

The results of in vivo studies indicate that vascular targeting of TNF is able to act in synergy with active or adoptive immunotherapy or chemotherapy, or both, against cancer.

Discussion

The results show that treatment of tumor-bearing mice with extremely low doses of NGR-TNF (5 ng/kg) is associated with a substantial modification of the cytokine-chemokine milieu of the tumor microenvironment and reverts EC anergy. These rapid and transient modifications favor the selective recruitment within the tumor mass, of fully activated endogenous or adoptively transferred CTL. Indeed, 2 h after NGR-TNF treatment, tumor-specific IFN-γ–producing CD8$^+$ T cells were already found to accumulate in the tumor mass, but not in the blood, spleen, or kidney of tumor-bearing mice. Remarkably, whereas the duration of the measured direct effects of NGR-TNF were short, the beneficial effects induced by NGR-TNF on TIL appeared to last for days. As a direct consequence, the therapeutic efficacy of both active and adoptive immunotherapies were significantly increased. Indeed, NGR-TNF treatment synergized with a DC-based vaccine given alone or in combination with DOXO, and in the context of two models of adoptive immunotherapy. While efficacious, the proposed combined therapies did not cause complete tumor regression, and the mice eventually succumbed to the tumor. Especially in the context of adoptive immunotherapy, the addition of exogenous cytokines, such as IL-2 and IL-15, or preconditioning of the

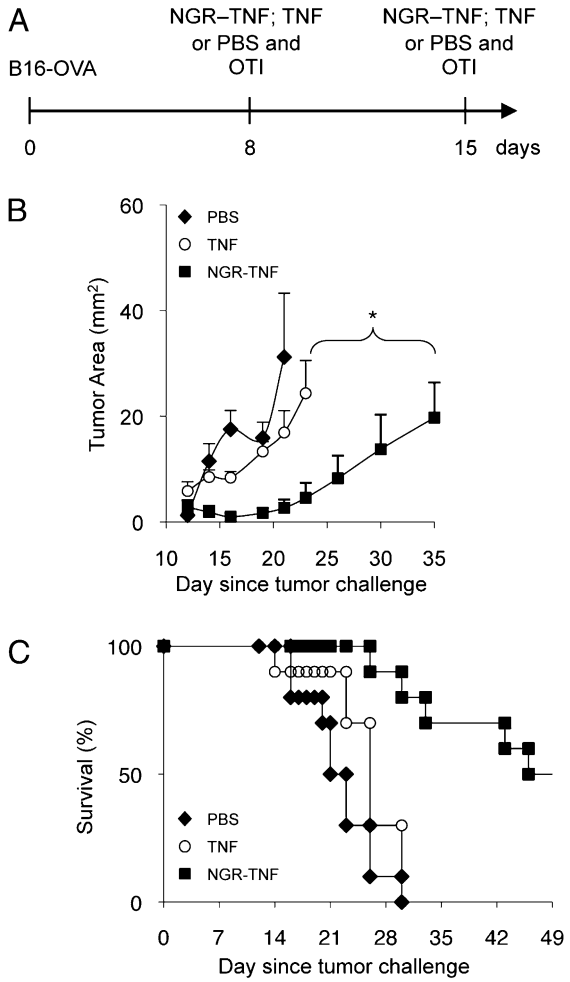

FIGURE 4. Adoptive immunotherapy combined with vascular targeting increases the survival of melanoma-bearing mice. (**A**) Schematic representation of the experiment. Mice bearing an 8-d-old B16-OVA melanoma were randomly assigned to either one of the following treatments (10 per group): PBS, NGR-TNF, or TNF followed 2 h later by activated OTI cells as described in Fig. 1. The same treatment was repeated 7 d later. Tumor growth was monitored twice per week for individual mice, and mice were killed when the mean tumor diameter was ≥10 mm or when the tumor became ulcerated. (**B**) Average tumor area (±SE) for each experimental group. Statistic analyses were performed at day 21 using the Student *t* test: PBS/OTI versus TNF/OTI, $p = 0.3$; PBS/OTI versus NGR-TNF/OTI, $p = 0.0318$; TNF/OTI versus NGR-TNF/OTI, $p = 0.0052$. The Student *t* test followed by Wilcoxon posttest was implemented for the comparison between NGR-TNF/OTI and TNF/OTI curves, $*0.01 < p < 0.05$. (**C**) Survival curves are reported in a Kaplan–Meier plot. Log rank tests: PBS/OTI versus TNF/OTI, $p = 0.18$; PBS/OTI versus NGR-TNF/OTI, $p < 0.0001$; TNF/OTI versus NGR-TNF/OTI, $p = 0.0002$.

recipient to favor proliferation of the transferred T cells would likely synergize with NGR-TNF based strategies (5). Further study is warranted to specifically address this issue.

The results of the studies on the mechanism of action show that a comparable dose of TNF was marginally or not active, thereby suggesting the hypothesis of an NGR-mediated targeting mechanism. One may wonder whether a targeting mechanism is indeed necessary for the local activity of TNF, or whether high-dose TNF can induce effects similar to those induced by low-dose (0.1 ng) NGR-TNF. We have shown previously that injection of 1–10 ng, but not 0.1 ng, of TNF or NGR-TNF to mice induces the shedding of soluble TNF receptors in circulation, a counterregulatory mechanism that inhibits most of TNF activity (15). Therefore, nanogram doses of both TNF and NGR-TNF (e.g., 10 ng) are almost inactive in murine models (15). Microgram doses of TNF can overcome the counterregulatory mechanisms, but also lead to toxic reactions (15). These data suggest that targeted delivery of low-dose NGR-TNF to tumor vessels is necessary and sufficient to induce local effects without inducing systemic counterregulatory mechanisms or toxic reactions. Given that NGR peptides recognize a CD13 isoform expressed by tumor vessels, this finding points to a vascular targeting mechanism. However, other cells in the tumor may express CD13, such as fibroblasts and pericytes; therefore, we cannot exclude that these cells also contribute to promote changes in the tumor microenvironment. We can also hypothesize a direct effect of the NGR–CD13 interaction on endothelial cells, which has not been investigated.

Remarkably, picogram doses of NGR-TNF caused a rapid upregulation of adhesion molecules on tumor ECs and local release of MCP-1/CCL-2, MCP-3/CCL-7, and MIP-2. MCP-1/CCL-2 is mainly produced by monocytes/macrophages, often together with MCP-3/CCL7, and also by endothelial cells, fibroblasts, and epithelial and smooth muscle cells. These chemokines regulate migration of monocytes, DCs, NK cells, and activated T cells (35, 36). MCP-1 has also a relevant role in the generation and survival of memory $CD8^+$ T cells and in the migration and function of adoptively transferred T cells, the latter function being impaired in MCP-$1^{-/-}$ mice (37). MIP-2 is mainly released from activated macrophages (38) and favors polymorphonuclear leukocyte recruitment. In addition, MIP-1β, RANTES, and lymphotactin were found to be upregulated, although not to a statistical significant level, in the tumor of NGR-TNF treated mice. These are generally cosecreted with IFN-γ by activated $CD8^+$ T cells (39) and are involved in T cell movements within the inflamed tissue and as chemoattractants and coactivators of macrophages (40). Therefore, it is likely that their redundant effects on lymphocyte migration acted in synergy on TIL after NGR-TNF treatment.

Considering that several of the adhesion molecules and chemokines induced by NGR-TNF in the tumor microenvironment can be exploited by different leukocyte populations for their extravasation (31), it is likely that other leukocyte populations are attracted within the tumor mass, as a consequence of NGR-TNF treatment, and participate in the modification of the tumor microenvironment, making it more favorable for lymphocyte infiltration and effector functions. These mechanisms might explain the improved response observed when immunotherapy was combined with NGR-TNF. An additional mechanism for this synergy could reside in the ability of TNF to activate DCs and to support a Th1-like response (8). In this therapeutic setting, tumor-specific vaccination would further boost the natural immune response against cancer, prevent tolerance induction, and favor persistence of memory tumor-specific T cells.

The potential effects of NGR-TNF on tumor infiltration by lymphocytes and response to immunotherapy might not be limited to the upregulation of leukocyte chemoattractant and adhesion molecules. Indeed, temporary reduction of the endothelial barrier function, which is another effect of NGR-TNF (14, 41), might facilitate leukocyte extravasation, as suggested by the heavy infiltrate of $CD3^+$ cells within the stroma of prostate tumors in TRAMP mice treated with NGR-TNF. This effect on the endothelial permeability could also explain the good synergy observed with the chemoimmunotherapy combination, as we have previously documented that NGR-TNF can promote the penetration of chemotherapeutic drugs in tumors (14, 16). Finally, NGR-TNF treatment can also transiently reduce hypoxic areas of lymphomas (41) and favor TIL proliferation and survival. Thus, NGR-TNF can exert multiple effects in tumors, all potentially cooper-

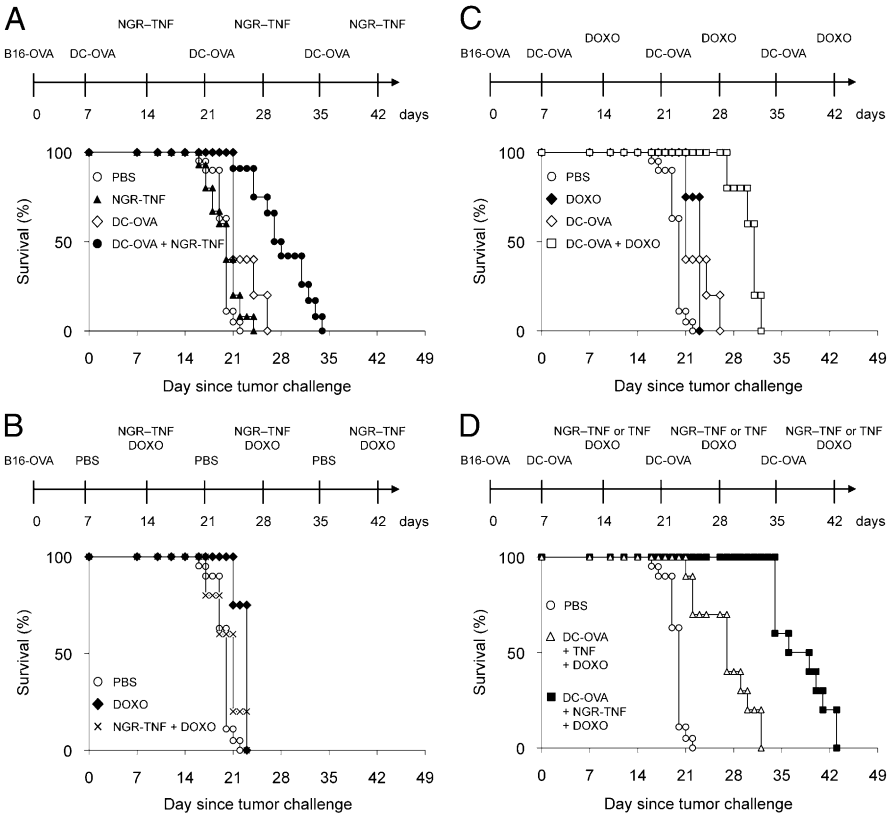

FIGURE 5. The combination of active immunotherapy, vascular targeting, and chemotherapy acts in synergy against melanoma. Mice bearing a palpable 8-d-old B16-OVA melanoma (5–21 per group) were randomly assigned to the following combined treatments: i.d. injection of DC-OVA (5×10^5 cells/mouse), i.p. injection of TNF or NGR-TNF (5 ng/kg), or i.p. injection of DOXO (4 mg/kg). As control, mice received i.d. or i.p. injections, or both, of PBS (100 μl/mouse). A schematic representation of the treatment schedule is reported at the *top of each panel*. Tumor growth was monitored twice per week for individual mice, and mice were killed when the mean tumor diameter was ≥15 mm or when the tumor became ulcerated. (**A–D**) Survival curves are reported in Kaplan–Meier plots. Log-rank tests: (A) PBS versus NGR-TNF, $p = 0.3$; PBS versus DC-OVA, $p = 0.009$; PBS versus DC-OVA plus NGR-TNF, $p < 0.0001$; DC-OVA versus DC-OVA plus NGR-TNF, $p = 0.002$; NGR-TNF versus DC-OVA, $p = 0.08$; NGR-TNF versus DC-OVA plus NGR-TNF, $p < 0.0001$; (B) PBS versus NGR-TNF plus DOXO, $p = 0.15$; (C) PBS versus DOXO, $p = 0.002$; PBS versus DC-OVA plus DOXO, $p < 0.0001$; DOXO versus DC-OVA, $p = 0.81$; DOXO versus DC-OVA plus DOXO, $p < 0.0001$; DC-OVA versus DC-OVA plus DOXO, $p = 0.001$; (D) PBS versus DC-OVA plus NGR-TNF plus DOXO, $p < 0.0001$; PBS versus DC-OVA plus TNF plus DOXO, $p < 0.0001$; DC-OVA plus TNF plus DOXO versus DC-OVA plus NGR-TNF plus DOXO, $p < 0.0001$.

ating in the synergism with chemoimmunotherapy. Further study is necessary to assess what is predominant.

NGR-TNF is the first TNF derivative to be developed for its delivery to tumors and has shown antitumor efficacy in cancer patients (18, 19). In addition to NGR-TNF, other tumor vessel-homing derivatives of TNF could be exploited, in principle, for the same purpose. For example, TNF-fusion proteins with ACDCRGDCFCG or CisoDGRC peptides (both ligands of αv integrins) (42, 43), or with the single chain Fv Ab L19, directed against the extradomain B of fibronectin (44), might serve for the same purpose, because they also recognize target molecules that are expressed by the tumor neovasculature. However, given that the location of the target molecules in tumor vessels and their level of expression are different from that of CD13 (the NGR receptor), further study is necessary to assess this hypothesis.

Lymphocyte infiltration in tumors can also be favored by the use of antiangiogenic compounds, such as anti-VEGF Abs (7, 45–47) that are also able to inhibit the formation of new blood vessels and promote vascular normalization (48). From a conceptual point of view, these strategies are different from that proposed in the current study, which exploits NGR-TNF as an inflammatory-vascular targeting agent that induces vascular activation. Notably, the use of antiangiogenic compounds requires higher doses of drugs and more frequent administration, possibly inducing greater toxic reactions. The observation that extremely low doses of NGR-TNF are sufficient to induce local tumor effects with no signs of systemic toxicity makes NGR-TNF a more attractive agent for its combination with immunotherapy and chemoimmunotherapy. In this regard, it is remarkable that most of the effects induced by NGR-TNF on the vessels of murine tumors (14–16) have been observed also in patients (18, 19). Therefore, association of NGR-TNF with current active and adoptive immunotherapies and chemoimmunotherapies appears to be a safe and efficacious strategy. This combination should concomitantly alter tumor vessel permeability and favor chemotherapeutic drug and leukocyte penetration, tumor cell death, inflammation, and tumor Ag cross presentation in peripheral lymphoid organs and at the tumor site. Furthermore, NGR-TNF might transiently decrease intratumoral hypoxia, rendering the tumor more susceptible to chemotherapy and immune-mediated attack. Our findings identify a novel property of NGR-TNF and could be relevant for the design of novel immunotherapeutic approaches for cancer patients.

Acknowledgments

We thank M.P. Protti and V. Russo (Istituto Scientifico San Raffaele, Milan, Italy) for helpful discussion and critical reading of the manuscript.

Disclosures

A. Corti is the inventor of a patent on NGR-TNF. The other authors have no financial conflicts of interest.

References

1. Rabinovich, G. A., D. Gabrilovich, and E. M. Sotomayor. 2007. Immunosuppressive strategies that are mediated by tumor cells. *Annu. Rev. Immunol.* 25: 267–296.
2. Chung, A. S., J. Lee, and N. Ferrara. 2010. Targeting the tumour vasculature: insights from physiological angiogenesis. *Nat. Rev. Cancer* 10: 505–514.
3. Piali, L., A. Fichtel, H. J. Terpe, B. A. Imhof, and R. H. Gisler. 1995. Endothelial vascular cell adhesion molecule 1 expression is suppressed by melanoma and carcinoma. *J. Exp. Med.* 181: 811–816.
4. Dougan, M., and G. Dranoff. 2009. Immune therapy for cancer. *Annu. Rev. Immunol.* 27: 83–117.
5. Rosenberg, S. A., N. P. Restifo, J. C. Yang, R. A. Morgan, and M. E. Dudley. 2008. Adoptive cell transfer: a clinical path to effective cancer immunotherapy. *Nat. Rev. Cancer* 8: 299–308.
6. Melder, R. J., G. C. Koenig, B. P. Witwer, N. Safabakhsh, L. L. Munn, and R. K. Jain. 1996. During angiogenesis, vascular endothelial growth factor and basic fibroblast growth factor regulate natural killer cell adhesion to tumor endothelium. *Nat. Med.* 2: 992–997.
7. Dirkx, A. E., M. G. Oude Egbrink, M. J. Kuijpers, S. T. van der Niet, V. V. Heijnen, J. C. Bouma-ter Steege, J. Wagstaff, and A. W. Griffioen. 2003. Tumor angiogenesis modulates leukocyte-vessel wall interactions in vivo by reducing endothelial adhesion molecule expression. *Cancer Res.* 63: 2322–2329.
8. Bemelmans, M. H., L. J. van Tits, and W. A. Buurman. 1996. Tumor necrosis factor: function, release and clearance. *Crit. Rev. Immunol.* 16: 1–11.
9. ten Hagen, T. L., A. L. Seynhaeve, and A. M. Eggermont. 2008. Tumor necrosis factor-mediated interactions between inflammatory response and tumor vascular bed. *Immunol. Rev.* 222: 299–315.
10. Corti, A., F. Curnis, W. Arap, and R. Pasqualini. 2008. The neovasculature homing motif NGR: more than meets the eye. *Blood* 112: 2628–2635.
11. Pasqualini, R., E. Koivunen, R. Kain, J. Lahdenranta, M. Sakamoto, A. Stryhn, R. A. Ashmun, L. H. Shapiro, W. Arap, and E. Ruoslahti. 2000. Aminopeptidase N is a receptor for tumor-homing peptides and a target for inhibiting angiogenesis. *Cancer Res.* 60: 722–727.
12. Curnis, F., G. Arrigoni, A. Sacchi, L. Fischetti, W. Arap, R. Pasqualini, and A. Corti. 2002. Differential binding of drugs containing the NGR motif to CD13 isoforms in tumor vessels, epithelia, and myeloid cells. *Cancer Res.* 62: 867–874.
13. Oostendorp, M., K. Douma, T. M. Hackeng, A. Dirksen, M. J. Post, M. A. van Zandvoort, and W. H. Backes. 2008. Quantitative molecular magnetic resonance imaging of tumor angiogenesis using cNGR-labeled paramagnetic quantum dots. *Cancer Res.* 68: 7676–7683.
14. Curnis, F., A. Sacchi, L. Borgna, F. Magni, A. Gasparri, and A. Corti. 2000. Enhancement of tumor necrosis factor alpha antitumor immunotherapeutic properties by targeted delivery to aminopeptidase N (CD13). *Nat. Biotechnol.* 18: 1185–1190.
15. Curnis, F., A. Sacchi, and A. Corti. 2002. Improving chemotherapeutic drug penetration in tumors by vascular targeting and barrier alteration. *J. Clin. Invest.* 110: 475–482.
16. Bertilaccio, M. T., M. Grioni, B. W. Sutherland, E. Degl'Innocenti, M. Freschi, E. Jachetti, N. M. Greenberg, A. Corti, and M. Bellone. 2008. Vasculature-targeted tumor necrosis factor-alpha increases the therapeutic index of doxorubicin against prostate cancer. *Prostate* 68: 1105–1115.
17. Dondossola, E., A. M. Gasparri, B. Colombo, A. Sacchi, F. Curnis, and A. Corti. 2011. Chromogranin A restricts drug penetration and limits the ability of NGR-TNF to enhance chemotherapeutic efficacy. *Cancer Res.* 71: 5881–5890.
18. Gregorc, V., A. Santoro, E. Bennicelli, C. J. Punt, G. Citterio, J. N. Timmer-Bonte, F. Caligaris Cappio, A. Lambiase, C. Bordignon, and C. M. van Herpen. 2009. Phase Ib study of NGR-hTNF, a selective vascular targeting agent, administered at low doses in combination with doxorubicin to patients with advanced solid tumours. *Br. J. Cancer* 101: 219–224.
19. Gregorc, V., P. A. Zucali, A. Santoro, G. L. Ceresoli, G. Citterio, T. M. De Pas, N. Zilembo, F. De Vincenzo, M. Simonelli, G. Rossoni, et al. 2010. Phase II study of asparagine-glycine-arginine-human tumor necrosis factor alpha, a selective vascular targeting agent, in previously treated patients with malignant pleural mesothelioma. *J. Clin. Oncol.* 28: 2604–2611.
20. Greenberg, N. M., F. DeMayo, M. J. Finegold, D. Medina, W. D. Tilley, J. O. Aspinall, G. R. Cunha, A. A. Donjacour, R. J. Matusik, and J. M. Rosen. 1995. Prostate cancer in a transgenic mouse. *Proc. Natl. Acad. Sci. USA* 92: 3439–3443.
21. Hogquist, K. A., S. C. Jameson, W. R. Heath, J. L. Howard, M. J. Bevan, and F. R. Carbone. 1994. T cell receptor antagonist peptides induce positive selection. *Cell* 76: 17–27.
22. Mombaerts, P., J. Iacomini, R. S. Johnson, K. Herrup, S. Tonegawa, and V. E. Papaioannou. 1992. RAG-1-deficient mice have no mature B and T lymphocytes. *Cell* 68: 869–877.
23. Bellone, M., D. Cantarella, P. Castiglioni, M. C. Crosti, A. Ronchetti, M. Moro, M. P. Garancini, G. Casorati, and P. Dellabona. 2000. Relevance of the tumor antigen in the validation of three vaccination strategies for melanoma. *J. Immunol.* 165: 2651–2656.
24. Ljunggren, H. G., and K. Kärre. 1985. Host resistance directed selectively against H-2-deficient lymphoma variants. Analysis of the mechanism. *J. Exp. Med.* 162: 1745–1759.
25. Iezzi, G., A. Boni, E. Degl'Innocenti, M. Grioni, M. T. Bertilaccio, and M. Bellone. 2006. Type 2 cytotoxic T lymphocytes modulate the activity of dendritic cells toward type 2 immune responses. *J. Immunol.* 177: 2131–2137.
26. Camporeale, A., A. Boni, G. Iezzi, E. Degl'Innocenti, M. Grioni, A. Mondino, and M. Bellone. 2003. Critical impact of the kinetics of dendritic cells activation on the in vivo induction of tumor-specific T lymphocytes. *Cancer Res.* 63: 3688–3694.
27. Boni, A., G. Iezzi, E. Degl'Innocenti, M. Grioni, E. Jachetti, A. Camporeale, and M. Bellone. 2006. Prolonged exposure of dendritic cells to maturation stimuli favors the induction of type-2 cytotoxic T lymphocytes. *Eur. J. Immunol.* 36: 3157–3166.
28. Hess Michelini, R., M. Freschi, T. Manzo, E. Jachetti, E. Degl'Innocenti, M. Grioni, V. Basso, C. Bonini, E. Simpson, A. Mondino, and M. Bellone. 2010. Concomitant tumor and minor histocompatibility antigen-specific immunity initiate rejection and maintain remission from established spontaneous solid tumors. *Cancer Res.* 70: 3505–3514.
29. Curnis, F., and A. Corti. 2004. Production and characterization of recombinant human and murine TNF. *Methods Mol. Med.* 98: 9–22.
30. Curnis, F., A. Cattaneo, R. Longhi, A. Sacchi, A. M. Gasparri, F. Pastorino, P. Di Matteo, C. Traversari, A. Bachi, M. Ponzoni, et al. 2010. Critical role of flanking residues in NGR-to-isoDGR transition and CD13/integrin receptor switching. *J. Biol. Chem.* 285: 9114–9123.
31. Pribila, J. T., A. C. Quale, K. L. Mueller, and Y. Shimizu. 2004. Integrins and T cell-mediated immunity. *Annu. Rev. Immunol.* 22: 157–180.
32. Lugade, A. A., J. P. Moran, S. A. Gerber, R. C. Rose, J. G. Frelinger, and E. M. Lord. 2005. Local radiation therapy of B16 melanoma tumors increases the generation of tumor antigen-specific effector cells that traffic to the tumor. *J. Immunol.* 174: 7516–7523.
33. Degl'Innocenti, E., M. Grioni, A. Boni, A. Camporeale, M. T. Bertilaccio, M. Freschi, A. Monno, C. Arcelloni, N. M. Greenberg, and M. Bellone. 2005. Peripheral T cell tolerance occurs early during spontaneous prostate cancer development and can be rescued by dendritic cell immunization. *Eur. J. Immunol.* 35: 66–75.
34. Casati, A., V. S. Zimmermann, F. Benigni, M. T. Bertilaccio, M. Bellone, and A. Mondino. 2005. The immunogenicity of dendritic cell-based vaccines is not hampered by doxorubicin and melphalan administration. *J. Immunol.* 174: 3317–3325.
35. Deshmane, S. L., S. Kremlev, S. Amini, and B. E. Sawaya. 2009. Monocyte chemoattractant protein-1 (MCP-1): an overview. *J. Interferon Cytokine Res.* 29: 313–326.
36. Proost, P., A. Wuyts, and J. Van Damme. 1996. Human monocyte chemotactic proteins-2 and -3: structural and functional comparison with MCP-1. *J. Leukoc. Biol.* 59: 67–74.
37. Wang, T., H. Dai, N. Wan, Y. Moore, and Z. Dai. 2008. The role for monocyte chemoattractant protein-1 in the generation and function of memory CD8+ T cells. *J. Immunol.* 180: 2886–2893.
38. Wolpe, S. D., B. Sherry, D. Juers, G. Davatelis, R. W. Yurt, and A. Cerami. 1989. Identification and characterization of macrophage inflammatory protein 2. *Proc. Natl. Acad. Sci. USA* 86: 612–616.
39. Dorner, B. G., A. Scheffold, M. S. Rolph, M. B. Huser, S. H. Kaufmann, A. Radbruch, I. E. Flesch, and R. A. Kroczek. 2002. MIP-1alpha, MIP-1beta, RANTES, and ATAC/lymphotactin function together with IFN-gamma as type 1 cytokines. *Proc. Natl. Acad. Sci. USA* 99: 6181–6186.
40. Ordway, D., D. M. Higgins, J. Sanchez-Campillo, J. S. Spencer, M. Henao-Tamayo, M. Harton, I. M. Orme, and M. Gonzalez Juarrero. 2007. XCL1 (lymphotactin) chemokine produced by activated CD8 T cells during the chronic stage of infection with *Mycobacterium tuberculosis* negatively affects production of IFN-gamma by CD4 T cells and participates in granuloma stability. *J. Leukoc. Biol.* 82: 1221–1229.
41. van Laarhoven, H. W., G. Gambarota, A. Heerschap, J. Lok, I. Verhagen, A. Corti, S. Toma, C. Gallo Stampino, A. van der Kogel, and C. J. Punt. 2006. Effects of the tumor vasculature targeting agent NGR-TNF on the tumor microenvironment in murine lymphomas. *Invest. New Drugs* 24: 27–36.
42. Curnis, F., A. Gasparri, A. Sacchi, A. Cattaneo, F. Magni, and A. Corti. 2005. Targeted delivery of IFNgamma to tumor vessels uncouples antitumor from counterregulatory mechanisms. *Cancer Res.* 65: 2906–2913.
43. Curnis, F., A. Sacchi, A. Gasparri, R. Longhi, A. Bachi, C. Doglioni, C. Bordignon, C. Traversari, G. P. Rizzardi, and A. Corti. 2008. Isoaspartate-glycine-arginine: a new tumor vasculature-targeting motif. *Cancer Res.* 68: 7073–7082.
44. Borsi, L., E. Balza, B. Carnemolla, F. Sassi, P. Castellani, A. Berndt, H. Kosmehl, A. Biro, A. Siri, P. Orecchia, et al. 2003. Selective targeted delivery of TNFalpha to tumor blood vessels. *Blood* 102: 4384–4392.
45. Li, B., A. S. Lalani, T. C. Harding, B. Luan, K. Koprivnikar, G. Huan Tu, R. Prell, M. J. VanRoey, A. D. Simmons, and K. Jooss. 2006. Vascular endothelial growth factor blockade reduces intratumoral regulatory T cells and enhances the efficacy of a GM-CSF-secreting cancer immunotherapy. *Clin. Cancer Res.* 12: 6808–6816.
46. Shrimali, R. K., Z. Yu, M. R. Theoret, D. Chinnasamy, N. P. Restifo, and S. A. Rosenberg. 2010. Antiangiogenic agents can increase lymphocyte infiltration into tumor and enhance the effectiveness of adoptive immunotherapy of cancer. *Cancer Res.* 70: 6171–6180.
47. Podar, K., and K. C. Anderson. 2005. The pathophysiologic role of VEGF in hematologic malignancies: therapeutic implications. *Blood* 105: 1383–1395.
48. Jain, R. K. 2005. Normalization of tumor vasculature: an emerging concept in antiangiogenic therapy. *Science* 307: 58–62.